

# Structural phase transitions in geometrically frustrated antiferromagnets

T. E. Saunders and J. T. Chalker

*Theoretical Physics, University of Oxford, 1 Keble Road, Oxford, OX1 3NP, United Kingdom*

(Dated: September 4, 2021)

We study geometrically frustrated antiferromagnets with magnetoelastic coupling. Frustration in these systems may be relieved by a structural transition to a low temperature phase with reduced lattice symmetry. We examine the statistical mechanics of this transition and the effects on it of quenched disorder, using Monte Carlo simulations of the classical Heisenberg model on the pyrochlore lattice with coupling to uniform lattice distortions. The model has a transition between a cubic, paramagnetic high-temperature phase and a tetragonal, Néel ordered low-temperature phase. It does not support the spin-Peierls phase, which is predicted as an additional possibility within Landau theory, and the transition is first-order for reasons unconnected with the symmetry analysis of Landau theory. Quenched disorder stabilises the cubic phase, and we find a phase diagram as a function of temperature and disorder strength similar to that observed in  $\text{Zn}_{1-x}\text{Cd}_x\text{Cr}_2\text{O}_4$ .

PACS numbers: 75.10.Hk 75.10.Nr 75.50.Lk

## I. INTRODUCTION

Much of the interesting behaviour observed in geometrically frustrated antiferromagnets<sup>1</sup> can be related to macroscopic ground state degeneracy in classical models for these systems. Some of the simplest models, with only nearest neighbour exchange interactions, remain in the paramagnetic phase down to zero temperature.<sup>2,3,4</sup> Characterising the strength of exchange interactions by the magnitude of the Curie-Weiss constant  $\Theta_{\text{CW}}$ , the paramagnetic phase is strongly correlated at temperatures  $T \ll |\Theta_{\text{CW}}|$ . More realistically, ground state degeneracy is lifted by additional interactions or coupling between spins and other degrees of freedom. As a result, the magnet may order or freeze at a temperature  $T_c$ . If the relevant energy scales are small compared to exchange,  $T_c \ll |\Theta_{\text{CW}}|$ . One such escape route from the strongly correlated paramagnet arises from magnetoelastic coupling, which may lead to a magnetically driven cooperative Jahn-Teller transition.<sup>5,6,7,8</sup> An alternative is that weak quenched disorder leads to spin freezing at low temperature.<sup>9</sup> In this paper we study structural phase transitions induced by magnetoelastic coupling in geometrically frustrated antiferromagnets and their suppression by quenched disorder.

Recent theoretical work<sup>6,7,8</sup> on magnetic Jahn-Teller transitions in geometrically frustrated magnets has combined an exact treatment of a tetrahedral cluster of four spins with Landau theory applied to the pyrochlore lattice. Results for the cluster show that arbitrarily weak magnetoelastic coupling generates an instability to a distorted ground state. Landau theory elevates this instability to an ordering transition, with several possible phase diagrams.<sup>7,8</sup> Depending on the distortion mode, the transition from the cubic, paramagnetic phase to a tetragonal phase may be a continuous one, or it may be first order. If the transition is continuous, then spin Peierls order is expected in the tetragonal phase immediately below the critical point, but may give way to Néel order at lower temperature. Alternatively, if the cubic to tetragonal

transition is discontinuous, it may either be to a phase with spin Peierls order, or directly to one with Néel order.

While Landau theory provides an exhaustive listing of possibilities, a microscopic approach is necessary to decide which occur in a given model. Moreover, it may happen that transitions which on symmetry grounds need not be first order, because there is no cubic invariant in the Landau expansion for the free energy, in fact are discontinuous, because a fourth-order invariant has a negative coefficient. These considerations motivate the work we describe here.

We examine as a representative model the classical Heisenberg antiferromagnet with nearest neighbour exchange interactions on the pyrochlore lattice, including magnetoelastic coupling to distortions from cubic to tetragonal symmetry. Ordering occurs if a lattice distortion is accompanied by a free energy gain in the spin system that outweighs its cost in elastic energy. The ordering temperature  $T_c$  depends on the strength of the magnetoelastic coupling compared to the appropriate elastic modulus. If coupling is weak,  $T_c \ll |\Theta_{\text{CW}}|$ . In the weak-coupling regime, thermodynamic behaviour is independent of the strength of exchange interactions and a universal function of the ratio  $T/T_c$ . We investigate the balance between magnetic free energy and elastic energy in this regime by using Monte Carlo simulations of the spin system to provide a numerically exact treatment of its statistical mechanics. We combine this with a mean field treatment of the lattice degrees of freedom, in which we allow only uniform lattice distortions. We believe our approach brings the advantages of a microscopic treatment of the magnetic degrees of freedom that drive ordering, without the complications and additional parameters that would arise in a full treatment of phonons.

Our results establish a rather different picture of the magnetic Jahn-Teller transition from that suggested previously. We find that the structural transition is strongly first order, and to a Néel ordered state, independently of any cubic invariant in the elastic energy. In this sense, the transition is driven by the energy gain arising from

Néel order, and not from spin Peierls order. Since the jump we observe in the Néel order parameter is large, we believe this conclusion is likely to be robust, even though a change in microscopic details of the model may in principle favour spin Peierls order.

The fact that arbitrarily weak magnetoelastic coupling is sufficient to generate a ground state instability prompts one to ask why structural phase transitions are not ubiquitous in geometrically frustrated antiferromagnets. We suggest here that weak exchange disorder (which is generated by random strains in the presence of magnetoelastic coupling) acts to stabilise the high symmetry lattice structure. As we have shown elsewhere, in the absence of a structural transition, there is spin glass ordering.<sup>9</sup> In this sense, the magnetic Jahn-Teller and spin glass transitions are alternative low-temperature fates for a geometrically frustrated antiferromagnet.

The remainder of the paper is organised as follows. In Sec. II we define our model and summarise our main conclusions. We present a Monte Carlo study of the thermally-driven transition in a clean system in Sec. III, and consider the disorder-driven transition at zero temperature in Sec. IV. Finally, in Sec. V we discuss our results in relation to experiments on  $\text{Zn}_{1-x}\text{Cd}_x\text{Cr}_2\text{O}_4$ .

## II. MODEL AND SUMMARY OF RESULTS

The model we treat has degrees of freedom of two types: classical Heisenberg spins  $\mathbf{S}_i$  of unit magnitude at the sites  $i$  of a pyrochlore lattice; and a uniform tetragonal distortion of this lattice, parameterised by a single variable  $\Delta$ . We include four contributions to the energy of the system: the exchange energy  $\mathcal{H}_0$  of the undistorted lattice; the change in exchange energy  $\mathcal{H}_\Delta$  due to magnetoelastic coupling; the elastic energy  $\mathcal{H}_{\text{el}}$ ; and the energy  $\mathcal{H}_{\text{dis}}$  arising from quenched exchange disorder.

With interaction strength  $J$  the exchange energy of the cubic pyrochlore lattice is

$$\mathcal{H}_0 = J \sum_{ij} \mathbf{S}_i \cdot \mathbf{S}_j, \quad (1)$$

where the sum is over nearest neighbour pairs. This Hamiltonian by itself is known to have a macroscopically degenerate ground state and to remain in the paramagnetic phase down to  $T = 0$ .<sup>3,4</sup> Our concern here is to find how other interactions lift this degeneracy and induce low temperature phase transitions.

We express the change in exchange energy due to magnetoelastic coupling in terms of the variable  $\Delta$ . For definiteness, we take the lattice distortion to be a compression of the cubic  $z$  axis and an expansion of the  $x$  and  $y$  axes. We characterise the amplitude of this distortion by its effect on exchange interactions, taking the interaction strength in the distorted system to be  $J - \Delta$  between neighbouring spin pairs in the same  $x$ - $y$  plane, and  $J + \Delta/2$  between pairs in adjacent  $x$ - $y$  planes. Then the

magnetoelastic coupling is

$$\mathcal{H}_\Delta = \sum_{ij} \Delta_{ij} \mathbf{S}_i \cdot \mathbf{S}_j, \quad (2)$$

where  $\Delta_{ij}$  has the values  $-\Delta$  and  $\Delta/2$  for pairs  $i, j$  of the two types. The ground states of  $\mathcal{H}_0 + \mathcal{H}_\Delta$  for  $\Delta > 0$  are Néel ordered: all spins in each  $x$ - $y$  plane of the lattice are ferromagnetically aligned, with opposite orientations on successive planes, as illustrated in Fig. 1. (The opposite choice of sign,  $\Delta < 0$ , leads to classical ground states with high degeneracy, and we do not consider it further.)

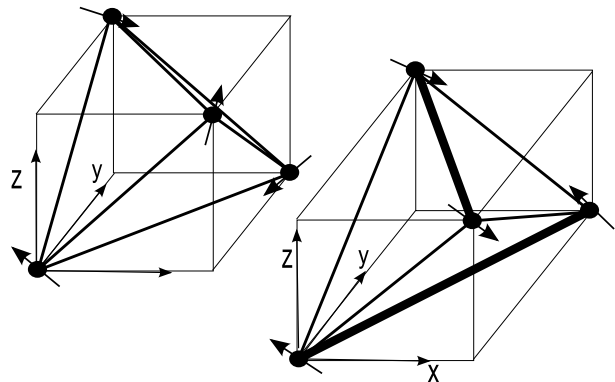


FIG. 1: Classical groundstate spin configurations on a single tetrahedron. Left: for an undistorted tetrahedron all exchange interactions are of equal strength and ground states include non-collinear spin configurations as illustrated. Right: for a tetragonally distorted tetrahedron, two longer bonds (broad lines) and four shorter bonds result in modulated interaction strengths, and ground state spin configurations are collinear.

We include elastic energy within a harmonic approximation, writing for a system of  $N$  spins

$$\mathcal{H}_{\text{el}} = \frac{\kappa}{2} N \Delta^2. \quad (3)$$

The coupling constant  $\kappa$  is related to an elastic coefficient  $c$  and the derivative  $\partial J / \partial x$  of exchange interaction strength with distance in the following way. First,  $\Delta$  can be expressed in terms of a strain  $\epsilon$  and an equilibrium bond length  $a$ , as the product  $\Delta = \epsilon a \partial J / \partial x$ . Taking the elastic energy density to be  $c\epsilon^2/2$ , we obtain Eq. (3) with  $\kappa \sim ca / (\partial J / \partial x)^2$ . Thus  $\kappa$  is large if magnetoelastic coupling is weak.

Exchange disorder is represented by

$$\mathcal{H}_{\text{dis}} = \sum_{ij} \delta_{ij} \mathbf{S}_i \cdot \mathbf{S}_j \quad (4)$$

with  $\delta_{ij}$  non-zero only for nearest neighbours, and drawn independently for each such pair  $i, j$  from a distribution that is uniform over the range  $[-\delta, \delta]$ .

Our objective is to study the model defined by the Hamiltonian

$$\mathcal{H} = \mathcal{H}_0 + \mathcal{H}_\Delta + \mathcal{H}_{\text{el}} + \mathcal{H}_{\text{dis}} \quad (5)$$

in the regime  $\kappa \gg J^{-1}$  and  $\Delta, \delta \ll J$ . In these circumstances  $\mathcal{H}_0$  makes the dominant contribution to the energy of the system and transitions from the paramagnetic phase take place at temperatures  $T \ll J$  (we set  $k_B = 1$  throughout this paper). In Fig. 2 we show a schematic phase diagram for the model as a function of the dimensionless variables  $\kappa T$  and  $\kappa \delta$ , which we now discuss. First, consider the system without quenched disorder ( $\delta = 0$ ) and at  $T = 0$ . Ground states are Néel ordered for  $\Delta > 0$  and in these states  $\mathcal{H}_\Delta = -2N\Delta$ . As a result,  $\mathcal{H}$  is minimised by a non-zero tetragonal lattice distortion, with  $\Delta = 2/\kappa$ , no matter how weak the magnetoelastic coupling and hence how large the coefficient  $\kappa$ . The net energy gain per spin from this lattice distortion is  $2/\kappa$ , and so one expects a transition to the paramagnetic phase at a temperature  $T_c \sim \kappa^{-1}$ . As we demonstrate in Sec. III, this transition is first order. Second, consider disruption of Néel order by exchange randomness at  $T = 0$ . Strong disorder leads to a larger modulation of exchange interactions than that produced by a uniform lattice distortion. In turn, this results in ground states with spin configurations that are random rather than Néel ordered, and an energy that is minimised at  $\Delta = 0$ . The transition from the Néel ordered state takes place at  $\delta \sim \kappa^{-1}$ . We show in Sec. IV that it is probably continuous. Finally, consider the effect of non-zero temperature at strong disorder. We have studied the model without magnetoelastic coupling ( $\kappa \rightarrow \infty$ ) elsewhere, finding a phase transition from a spin-glass ordered low temperature phase to a paramagnetic high temperature phase, with a transition temperature  $T_g \sim \delta$ .<sup>9</sup> We include this phase boundary in Fig. 2, although we have not attempted to investigate the multicritical point at which the three phases meet.

### III. MAGNETICALLY-DRIVEN STRUCTURAL PHASE TRANSITION

In this section we discuss the thermally driven transition in a system without disorder, between a high temperature, cubic, paramagnetic phase and a low-temperature, tetragonal phase, which we will show is Néel ordered. We restrict our attention to the regime of weak magnetoelastic coupling,  $\kappa \gg J^{-1}$ , in which behaviour depends only on the variable  $\kappa T$  and is independent of  $J$ . Our main tool is the use of Monte Carlo simulations to determine the free energy of the spin system.

Let  $F(\Delta, T)$  be the free energy per spin at temperature  $T$ , calculated from the Hamiltonian  $\mathcal{H}_0 + \mathcal{H}_\Delta$ . The combination

$$\Gamma(\Delta, T) = \frac{\mathcal{H}_{\text{el}}}{N} + F(\Delta, T) - F(0, T) \quad (6)$$

is the net free energy gain per spin arising from a lattice distortion. The physical value of  $\Delta$  is the one that minimises  $\Gamma(\Delta, T)$ , and the system is in a tetragonal phase if there is a value of  $\Delta > 0$  for which  $\Gamma(\Delta, T) < 0$ .

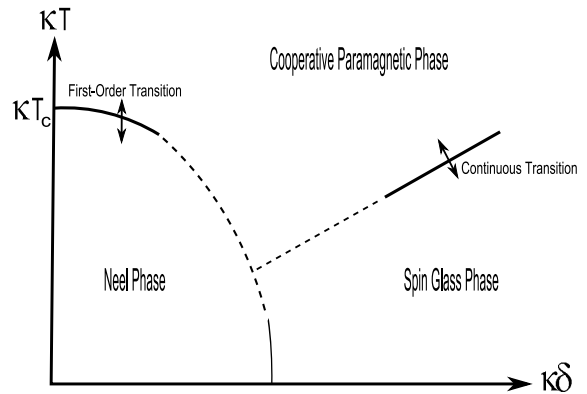


FIG. 2: Schematic phase diagram in the plane of scaled temperature  $\kappa T$  and disorder strength  $\kappa \delta$ , based on numerical simulations of (5).  $T_c$  denotes the temperature of a transition between a Néel ordered, tetragonal low temperature phase, and a paramagnetic, high temperature phase in the pure system. A similar transition occurs at zero temperature, at a disorder strength  $\delta_c$ . Solid lines represent phase boundaries that have been probed in simulations. Dashed lines are guides to the eye.

The contribution of the spin degrees of freedom to this free energy for  $T, \Delta \ll J$  can be written in the scaling form

$$F(\Delta, T) - F(0, T) = \Delta f_s(\Delta/T), \quad (7)$$

since in this regime  $\Delta$  sets the only energy scale for the spin system. The function  $f_s(x)$  plays an important role in the following, and it is useful to discuss its low and high temperature asymptotics. At low temperature ( $x \gg 1$ ) the magnetic free energy difference is dominated by the energy gain  $2\Delta$  per spin in the Néel state, and so  $\lim_{x \rightarrow \infty} f_s(x) = -2$ . Conversely, a high-temperature expansion (covering the regime  $1 \ll \kappa T \ll \kappa J$ ) gives for small  $x$

$$N\Delta f_s(\Delta/T) = \langle \mathcal{H}_\Delta \rangle_0 - \frac{1}{2T} [ \langle (\mathcal{H}_\Delta)^2 \rangle_0 - \langle \mathcal{H}_\Delta \rangle_0^2 ] + \mathcal{O}(\Delta^3/T^2), \quad (8)$$

where  $\langle \dots \rangle_0$  denotes an average with the Hamiltonian  $\mathcal{H}_0$  in the limit  $T \ll J$ . This average yields  $\langle \mathcal{H}_\Delta \rangle_0 = 0$  and  $\langle \mathcal{H}_\Delta^2 \rangle_0 = bN\Delta^2$  with  $b > 0$ , and so  $f_s(x) \sim -bx/2$  for  $x \rightarrow 0$ .

Now Eq. (6) can be written in terms of  $f_s(x)$  as

$$\begin{aligned} \Gamma(\Delta, T) &= \frac{\kappa}{2} \Delta^2 + \Delta f_s(\Delta/T) \\ &= T \left[ \frac{\kappa T}{2} x^2 + x f_s(x) \right]. \end{aligned} \quad (9)$$

The form of the function  $f_s(x)$  determines the critical point  $\kappa T_c$  and the order of the transition. The equation  $\kappa T x/2 + f_s(x) = 0$  has no solution for positive  $x$  in the

cubic phase ( $\kappa T > \kappa T_c$ ) but has a solution  $x_c > 0$  in the tetragonal phase. If  $x_c$  approaches zero as  $\kappa T$  approaches  $\kappa T_c$  from below, the transition is continuous, while if  $x_c$  remains finite in this limit, the transition is first order. Thus, the transition is continuous if  $f_s(x)$  is convex for  $0 < x < \infty$ ; otherwise it is first order.

### A. Numerical Approach

To find the magnetic free energy difference between the cubic and tetragonal phases, and specifically the function  $f_s(x)$ , we use Monte Carlo simulations of a spin system with the Hamiltonian  $\mathcal{H}_0 + \mathcal{H}_\Delta$ . The system simulated had the shape of a rhombohedron, with edges parallel to the primitive basis vectors of the lattice and with periodic boundary conditions. We focus on the temperature range  $T \ll J$  for fixed  $\Delta \ll J$  and ensure equilibration at low temperature by employing parallel tempering.<sup>10</sup> Representative simulation parameters are  $\Delta/J = 10^{-3}$  and  $T/J \geq 10^{-4}$ , with system sizes  $32 \leq N \leq 2048$  and measurement run lengths of up to  $2 \times 10^5$  parallel tempering steps, preceded by equilibration for the same number of steps. Within the parallel tempering algorithm spin configurations are exchanged amongst a range of possible temperatures: we checked in particular that each configuration explored all temperatures across an interval that spanned the first-order transition temperature. The data presented here are predominantly for systems of 500 and 864 spins, but larger system sizes were also simulated to ensure that finite size effects are not significant.

Determination of the free energy requires calculation of the entropy  $S(T)$ . We do this by integration of the heat capacity  $C_v(T)$ , using

$$S(T_0) - S(T) = \int_T^{T_0} \frac{C_v(T)}{T} dT \quad (10)$$

and choosing the reference temperature  $T_0 \gg \Delta$  so that  $S(T_0)$  is independent of  $\Delta$  and cancels from the free energy difference  $F(\Delta, T) - F(0, T)$ . We note that since  $C_v(T)$  is constant at low temperature in our classical model,  $S(T)$  is logarithmically divergent as  $T \rightarrow 0$ , but the contribution  $-TS(T)$  to the free energy has no divergence. For fixed  $\Delta > 0$  the spin system has a Néel ordering transition, which is first order in the regime of interest,  $\Delta \ll J$ . Numerical integration of  $C_v(T)/T$  across this transition is difficult, because the latent heat of the transition appears in a finite system as a narrow spike in  $C_v(T)$ . We circumvent this difficulty by using two independent approaches to find the entropy change at the transition, and checking between them for consistency. One approach is direct integration, using spline fits of  $C_v(T)$  around the transition. The other is to use the change in internal energy at the transition to determine the latent heat and hence the entropy jump.

### B. Results

Results from simulations for the scaled free energy difference  $[F(\Delta, T) - F(0, T)]/\Delta$  and internal energy  $E$  per spin as a function of temperature are shown in Fig. 3. We discuss first the behaviour of  $E$ . For a system with  $\Delta = 0$  the ground state energy per spin is  $-J$ , and  $E$  increases linearly with  $T$  at low temperature, because  $C_v(T)$  is constant. For  $\Delta > 0$  the ground state energy per spin is reduced by  $2\Delta$ . For fixed  $\Delta$  there is a Néel transition, which takes place at  $T/\Delta \approx 3.1$ : at the transition the internal energy per spin increases abruptly and approaches its value in a system with  $\Delta = 0$ . Consider next the the free energy difference. It is also small in the high temperature phase. In contrast to the internal energy difference, the free energy difference is of course continuous through the transition. It grows with decreasing temperature below the transition.

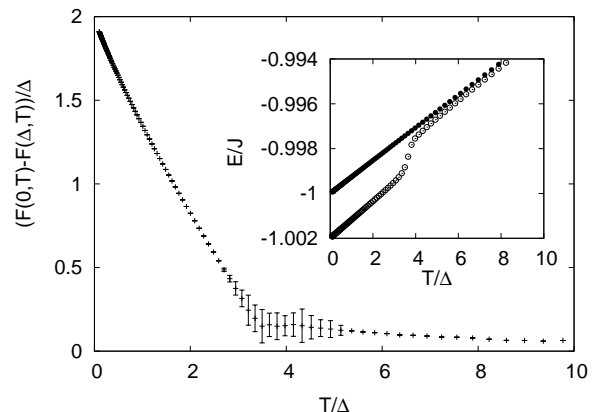


FIG. 3: Scaled free energy difference  $(F(0) - F(\Delta))/\Delta$  vs  $T/\Delta$  for  $\Delta/J = 10^{-3}$ . Inset: internal energy per spin on the same temperature scale, for  $\Delta/J = 10^{-3}$  (○) and  $\Delta = 0$  (●). All data for  $N = 256$  spins.

The free energy difference is replotted as a function of the variable  $x = \Delta/T$  in Fig. 4, together with the straight line through the origin that is tangent to the function  $f_s(x)$ . From the gradient of this line we identify the transition temperature  $T_c$  in the system with magnetoelastic coupling, obtaining  $\kappa T_c = 3.34$ . We also see that the transition is strongly first order, since the solution  $x_c \approx 0.60$  to the equation  $f_s(x) = -\kappa T_c x/2$  is finite. Note that the transition for the full model with Hamiltonian  $\mathcal{H}$ , in which the value of  $\Delta$  varies with  $T$  to minimise the free energy, preempts the one in a system with fixed  $\Delta$ . The latter transition is responsible for the kink in  $f_s(x)$ , visible at  $x \approx 0.3$  in Fig. 4. Of course, it is the extra elastic energy accompanying a lattice distortion that destabilises the Néel ordered state at a lower temperature in the full model than in the one with  $\Delta$  fixed.

To demonstrate that the tetragonal phase is indeed Néel ordered, we show in Fig. 5 the variation of the sub-

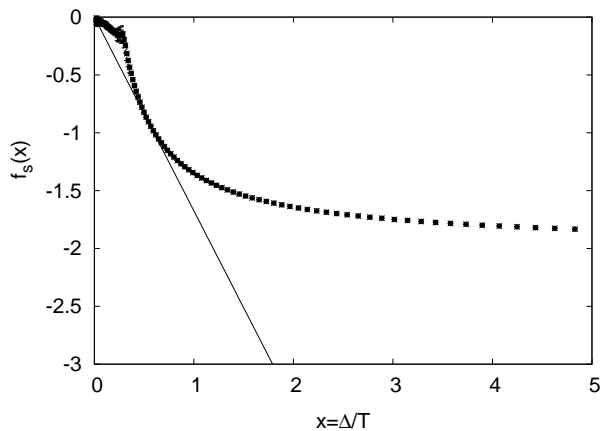


FIG. 4:  $f_s(x)$  vs  $x = \Delta/T$  for fixed  $\Delta/J = 10^{-3}$  ( $\bullet$ ). The straight line is tangent to  $f_s(x)$  and has gradient  $-1.67$ .

lattice magnetisation with temperature in a system with a fixed value of  $\Delta$ . At the critical point of the full model,  $T/\Delta \approx 1.7$  and the sublattice magnetisation is approximately 90% of its saturation value. We discuss the transition at fixed  $\Delta$  in detail elsewhere.<sup>11</sup>

In summary, the simple approach we have presented, which combines a microscopic treatment of the statistical mechanics of the spin degrees of freedom with mean field theory for the lattice distortion, yields a strongly first-order transition between cubic and tetragonal phases, with highly developed Néel order at all temperatures within the tetragonal phase. A first-order transition is also predicted using Landau theory, but the mechanism in that case is different: it arises because symmetry permits a term in the elastic energy which is cubic in strain. In our approach such a term would appear as a contribution to  $\mathcal{H}_{el}$  cubic in  $\Delta$ . Within Landau theory, first order transitions can arise in the absence of cubic invariants, if the expansion of the free energy in powers of the order parameter has a quartic term with a negative coefficient. This appears to be the mechanism that leads to the first order transition we find.

#### IV. INFLUENCE OF QUENCHED DISORDER

As we have seen, a structural phase transition is a generic feature of the model we have studied, irrespective of the strength of magnetoelastic coupling. The driving mechanism is the linear gain in exchange energy with lattice distortion for some ground state spin configurations of the high-symmetry structure. This magnetic Jahn-Teller mechanism is likely to apply to a variety of other classical models for geometrically frustrated magnets. Specifically, for it to be effective the set of ground states should include configurations in which  $\mathbf{S}_i \cdot \mathbf{S}_j$  takes different values for different nearest neighbour spin pairs, so that the exchange energy of the state varies linearly with lattice distortion  $\Delta$ . For example, this condition in-

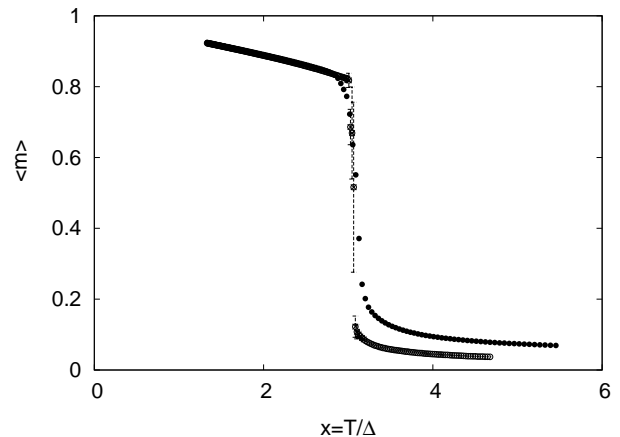


FIG. 5: Sublattice magnetisation  $m$  vs  $T/\Delta$  with  $\Delta/J = 10^{-3}$  for  $N = 864$  ( $\bullet$ ) and  $4000$  ( $\circ$ ). Errors only shown for  $N = 4000$  for clarity.

cludes Heisenberg model on the lattice appearing in the material SCGO,<sup>12</sup> but excludes the kagome Heisenberg antiferromagnet, in which  $\mathbf{S}_i \cdot \mathbf{S}_j = -1/2$  for all nearest neighbours in all ground states. In many materials, however, no structural transition is observed. Instead, geometrically frustrated magnets often show spin freezing at low temperature. Such freezing suggests the importance of residual disorder, even though samples in some cases appear to be almost disorder-free. In this section we examine how disorder may stabilise the cubic phase of our model. We present results obtained in two ways. First, we use Monte Carlo simulations to study a spin system with fixed  $\Delta > 0$  at various disorder strengths  $\delta$  as a function of temperature. We find that strong disorder suppresses the Néel transition that is observed at  $\delta = 0$ . Second, we examine behaviour at  $T = 0$  as a function of disorder strength, treating the dependence of ground state energy on  $\delta$  in the same way as we did the dependence of free energy on  $T$  in Sec. III.

##### A. Behaviour for $T > 0$ at fixed $\Delta$

The introduction of random exchange interactions complicates Monte Carlo simulations. Longer equilibration times are required (up to  $10^6$  parallel tempering steps) and we must average over disorder configurations. This limits the system sizes that can be simulated. The results we present were obtained for systems of size  $N = 864$ , averaging over 100 realisations for each disorder strength, with  $\Delta/J = 10^{-2}$ .

We show in Fig. 6 the heat capacity per spin as a function of temperature for various disorder strengths, expressed in terms of  $\Delta/\delta$  since we expect this ratio to control behaviour in the regime  $\Delta, \delta, T \ll J$ . We find that the sharp peak in heat capacity, associated at  $\delta = 0$  with a discontinuous Néel ordering transition, occurs at lower temperature with increasing disorder but persists

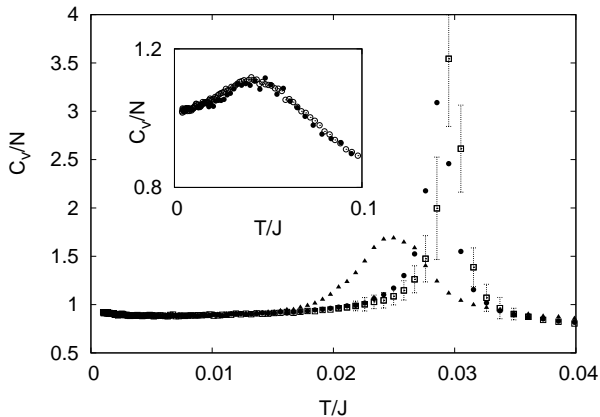


FIG. 6: Heat capacity per spin vs  $T/J$  for  $\Delta/\delta = 10$  ( $\square$ ),  $1$  ( $\bullet$ ), and  $0.5$  ( $\blacktriangle$ ) in a system of 864 spins at  $\Delta/J = 10^{-2}$ . Errors shown for system with largest error. Inset: heat capacity per spin vs  $T/J$  for 500 ( $\bullet$ ) and 864 ( $\circ$ ) spins at  $\Delta/\delta = 10^{-1}$  and  $\Delta/J = 10^{-2}$ . Errors indicated by scatter of points.

for  $\Delta/\delta \geq 1$ . At larger disorder strength,  $\Delta/\delta < 1$ , it is rounded, being smooth and independent of system size at  $\Delta/\delta = 10^{-1}$  (see inset to Fig. 6). The dominant errors are from disorder averaging. We conclude that the Néel transition is suppressed by disorder. It is presumably replaced at strong disorder by a spin glass transition, but because of the difficulties attached to Monte Carlo simulations in this regime, we do not investigate this further.

### B. Behaviour at $T = 0$

To make additional progress in quantifying the effect of disorder on the structural and magnetic phase transitions, we focus on behaviour at  $T=0$  as a function of  $\delta$ . Let  $E(\Delta, \delta)$  be the disorder-averaged ground state energy per spin for the spin system with Hamiltonian  $\mathcal{H}_0 + \mathcal{H}_\Delta + \mathcal{H}_{\text{dis}}$ . In analogy with Eq. (6), we define the energy combination

$$\Gamma_E(\Delta, \delta) = \frac{\mathcal{H}_{\text{el}}}{N} + E(\Delta, \delta) - E(0, \delta). \quad (11)$$

To determine the ground state lattice symmetry for a given disorder strength  $\delta$ , the value of  $\Delta$  should be chosen to minimise  $\Gamma_E(\Delta, \delta)$ . In the cubic phase the minimum is at  $\Delta = 0$ , while in the tetragonal phase it is at  $\Delta > 0$ .

We expect the spin contribution to this energy difference in the limit  $\Delta, \delta \ll J$  to have the scaling form

$$E(\Delta, \delta) - E(0, \delta) = \Delta f_E(\Delta/\delta) \quad (12)$$

with the asymptotic behaviour for  $f_E(y)$  given at large  $y$  by  $\lim_{y \rightarrow \infty} f_E(y) = -2$ , and at small  $y$  by  $f_E(y) \propto y$ . Using this scaling form

$$\Gamma_E(\Delta, \delta) = \Delta \left[ \frac{\kappa\delta}{2} y + f_E(y) \right]. \quad (13)$$

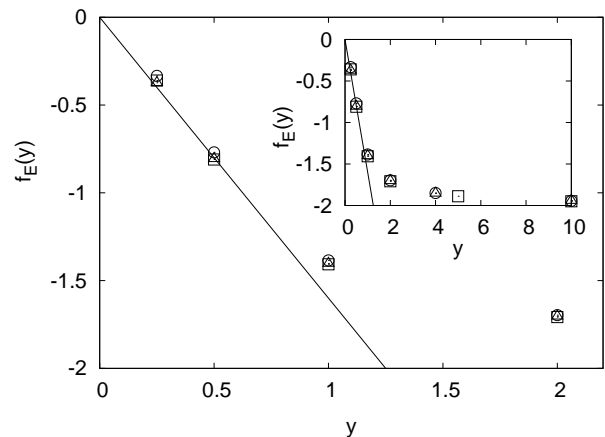


FIG. 7:  $f_E(y)$  vs  $y$  for three values of  $\Delta/J$ :  $10^{-1}$  ( $\circ$ ),  $10^{-2}$  ( $\diamond$ ) and  $5 \times 10^{-3}$  ( $\square$ ). The straight line is tangent to  $f_E(y)$  at  $y = 0$  and has gradient  $-\kappa\delta_c/2 = -1.6$ . The inset shows the same plot but for a larger range of  $y$ . Errors are less than the symbol sizes.

Thus the state of the system is controlled by the dimensionless coupling constant  $\kappa\delta$ . As for the thermally driven transition without disorder, there is a critical coupling  $\kappa\delta_c$ . If  $\kappa\delta > \kappa\delta_c$  the equation  $\kappa\delta y/2 + f_E(y) = 0$  has no solution for  $y > 0$  and the system is in the cubic phase. Alternatively, if  $\kappa\delta < \kappa\delta_c$  there is a solution at  $y_c > 0$  and the system is in the tetragonal phase. As for the thermally driven transition, the disorder-driven one is continuous if  $f_E(x)$  is convex for  $0 < x < \infty$  and first order otherwise.

We show in Fig. 7 the function  $f_E(y)$  determined numerically for a system of size  $N = 864$  spins, averaging over 50 disorder realisations. Low energy configurations are obtained by quenching low temperature states taken from Monte Carlo simulations using parallel tempering. The agreement between data for three values of  $\Delta/J$  demonstrates that the calculations are within the scaling regime  $\Delta, \delta \ll J$ . In contrast to behaviour at the thermally driven transition, it appears from the form of  $f_E(y)$  that  $y_c$  will approach zero smoothly as  $\kappa\delta$  approaches  $\kappa\delta_c$  from below. Hence the disorder driven, zero temperature transition is probably continuous. We find  $\kappa\delta_c = 3.2$ .

As a supplement to this study of the structural transition, we also examine the variation of sublattice magnetisation  $m$  with disorder strength at fixed  $\Delta$  in ground states. The sublattice magnetisation shows significant finite-size effects in our range of system sizes, and so we extrapolate to the limiting value  $m_\infty$  from results for  $N = 256, 500$  and  $864$ . We show the variation of  $m_\infty$  with  $y$  in Fig. 8, and the extrapolation in the inset. Sublattice magnetisation is not much affected by disorder for  $y > 1$ , and decreases to zero for  $y \approx 0.17$ . If it is indeed the case that  $f_E(y)$  is convex, so that the structural transition is continuous, and if it is also the case that the magnetisation is zero below a finite value of  $y$ , then the disorder driven, zero temperature transition is a

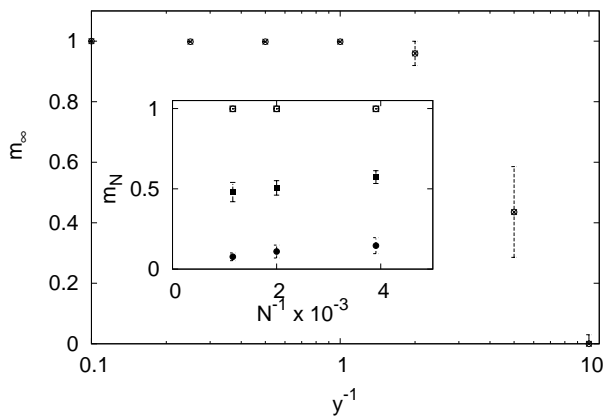


FIG. 8: Staggered magnetisation per spin in the infinite system vs  $y^{-1}$  on a logarithmic scale. Inset: illustration of the extrapolation of sublattice magnetisation  $m$  vs  $N^{-1}$  to infinite system size.

two-stage one, and there exists a tetragonal phase without Néel order at intermediate disorder strength. A more detailed investigation of this point would be demanding, and we do not pursue it.

### C. Paramagnetic-Spin Glass Phase Transition

We have not investigated the regime  $\kappa\delta \gg 1$  as part of the present work, but we draw attention to earlier studies of the effect of weak disorder ( $\delta \ll J$ ) at  $\Delta = 0$  (in effect,  $\kappa \rightarrow \infty$ ).<sup>9,13</sup> A continuous phase transition between the paramagnetic and spin glass phases occurs at a temperature proportional to  $\delta$ .<sup>9</sup>

## V. DISCUSSION

The model we have discussed provides a caricature for the chromium spinel oxides  $ACr_2O_4$ , where A is Mg,<sup>14</sup> Zn,<sup>5</sup> Cd,<sup>14</sup> or Hg.<sup>15</sup> These  $S = 3/2$  pyrochlore antiferromagnets undergo structural phase transitions accompanied by Néel ordering, with transition temperatures that are small compared to the magnitude of their Curie-Weiss constants. The structural distortions and magnetic ordering patterns are different in each compound and are considerably more complex than the one we have considered.<sup>15,16</sup> While we are therefore not able to make a detailed comparison with experiment, some qualitative

points deserve emphasis. These concern the mechanism driving the transition, the order of the transition, and the influence of non-magnetic impurities.

Our calculations demonstrate that, at least in the classical limit and for the uniform distortion mode we consider, the mechanism driving the structural transition is the energy gain from Néel order, rather than spin Peierls order. It is possible in principle that other distortion modes would allow a phase at intermediate temperature that has spin Peierls but no Néel order, but the very large discontinuity we observe in the Néel order parameter suggests to us that this is unlikely. It is also possible that quantum fluctuations favour spin Peierls order, and it would be interesting to attempt in future research to quantify this.

In addition, our results show that the phase transition can be first order for a reason unconnected to the symmetry analysis of Landau theory. This is significant because within Landau theory some structural distortion patterns are expected to lead to a first order transition while others should not. In particular, within Landau theory a transition involving a tetragonal distortion that is predominantly an odd mode (affecting the two tetrahedra in a unit cell oppositely) should be continuous, while a transition involving an even mode should be first order.<sup>7,8</sup> Our simulations demonstrate that a first order transition may result from a microscopic treatment, independently of expectations based on symmetry.

Finally, it is interesting to compare our study of the influence of exchange randomness on the transition with observations of the effect of non-magnetic impurities in the material  $Zn_{1-x}Cd_xCr_2O_4$ .<sup>17</sup> In this system a surprisingly small level of substitution ( $x = 0.03$ ) at non-magnetic sites is sufficient to suppress Néel order and the structural phase transition. The origin of this behaviour is believed to be the larger ionic radius of  $Cd^{2+}$  compared to  $Zn^{2+}$ : as a consequence, substitution leads to random strains, which in the presence of magnetoelastic coupling generate exchange randomness. The results we present in Sec. IV show this mechanism in action, and are qualitatively consistent with the phase diagram observed in  $Zn_{1-x}Cd_xCr_2O_4$  as a function of temperature and disorder strength, with  $x$  playing the role of our variable  $\delta$ .<sup>17</sup>

We thank P. C. W. Holdsworth, R. Moessner, and O. Tchernyshyov for valuable discussions. The work was supported in part by EPSRC Grant No. GR/R83712/01.

<sup>1</sup> For reviews, see: A. P. Ramirez, *Annu. Rev. Mater. Sci.* **24**, 453 (1994); P. Schiffer and A. P. Ramirez, *Comments Condens. Matter Phys.* **18**, 21 (1996).

<sup>2</sup> J. Villain, *Z. Phys. B* **33**, 31 (1979).

<sup>3</sup> J. N. Reimers, *Phys. Rev. B* **45**, 7287 (1992).

<sup>4</sup> R. Moessner and J. T. Chalker, *Phys. Rev. Lett.* **80**, 2929 (1998); R. Moessner and J. T. Chalker, *Phys. Rev. B* **58**,

12049 (1998).

<sup>5</sup> S.-H. Lee, C. Broholm, T. H. Kim, W. Ratcliff II, and S.-W. Cheong, *Phys. Rev. Lett.* **84**, 3718 (2000).

<sup>6</sup> Y. Yamashita and K. Ueda, *Phys. Rev. Lett.* **85**, 4960 (2000)

<sup>7</sup> O. Tchernyshyov, R. Moessner, and S. L. Sondhi, *Phys. Rev. Lett.* **88**, 067203 (2002).

- <sup>8</sup> O. Tchernyshyov, R. Moessner, and S. L. Sondhi, Phys. Rev. B **66**, 064403 (2002).
- <sup>9</sup> T. E. Saunders and J. T. Chalker, Phys. Rev. Lett. **98**, 157201 (2007).
- <sup>10</sup> K. Hukushima and K. Nemoto, J. Phys. Soc. Japan, **65**, 1604 (1996); for a review, see: E. Marinari in *Advances in Computer Simulation*, edited by J. Kertész and I. Kondor (Springer-Verlag, Berlin, 1998).
- <sup>11</sup> T. S. Pickles, T. E. Saunders, and J. T. Chalker, arXiv:0708.3791.
- <sup>12</sup> A. P. Ramirez, G. P. Espinosa, and A. S. Cooper, Phys. Rev. Lett. **64**, 2070 (1990).
- <sup>13</sup> L. Bellier-Castella, M. J. P. Gingras, P. C. W. Holdsworth, and R. Moessner, Can. J. Phys. **79**, 1365 (2001).
- <sup>14</sup> M. T. Rovers, P. P. Kyriakou, H. A. Dabkowska, G. M. Luke, M. I. Larkin, and A. T. Savici, Phys. Rev. B **66**, 174434 (2002).
- <sup>15</sup> H. Ueda, H. Mitamura, T. Goto, and Y. Ueda, Phys. Rev. B **73**, 094415 (2006).
- <sup>16</sup> S.-H. Lee, G. Gasparovic, C. Broholm, M. Matsuda, J.-H. Chung, Y. J. Kim, H. Ueda, G. Xu, P. Zschack, K. Kakurai, H. Takagi, W. Ratcliff, T. H. Kim, and S.-W. Cheong, J. Phys. Cond. Matt. **19**, 145259 (2007).
- <sup>17</sup> W. Ratcliff II, S.-H. Lee, C. Broholm, S.-W. Cheong and Q. Huang, Phys. Rev. B **65**, 220406(R) (2002).